A MONTE CARLO APPROACH TO DESCRIBE THE REDUCTION PROFILES OF BIDIMENSIONAL MoO_X STRUCTURES GROWN ON AN ALUMINA SUSTRATE

M. C. ABELLO[1*], A. P. VELASCO[2], O. A. FERRETTI[3] and J. L. G. FIERRO[4]

1 *INTEQUI, Instituto de Investigaciones en Tecnología Química (UNSL- CONICET), Chacabuco y Pedernera, 5700 San Luis, Argentina, e-mail: cabello@unsl.edu.ar*

2 Departamento de Física, Facultad de Ciencias Físico Matemáticas y Naturales (UNSL), Ejército de los Andes 950, 5700 San Luis, Argentina

3 CINDECA, Centro de Investigación y Desarrollo en Ciencias Aplicadas. Dr. Jorge Ronco (UNLP -CONICET) y Departamento de Ingeniería Química. (UNLP), 47 N° 257, 1900 La Plata, Argentina

4 Instituto de Catálisis y Petroleoquímica, CSIC, Cantoblanco, E-28049-Madrid, Spain

Abstract--The reducibility of molybdenum oxide supported on γ-Al_2O_3 was studied by temperature programmed reduction (TPR). Interpretation of the reduction profiles was successfully achieved by applying the Monte Carlo method and taking into account the presence of different molybdenum species on the support surface. Seven reactions were assumed to take place along the reduction process. The first hydrogen consumption peak was assigned to the reduction of Mo^{6+} ions present as well-dispersed polymeric species into Mo^{+5}, while the second one accounts for the reduction not of the Mo^{5+} ions generated in the first reduction into Mo^{+4} but also for the reduction of monomeric Mo^{6+} species.

***Keywords*— Mo catalysts; Monte Carlo method, Temperature programmed reduction.**

I. INTRODUCTION

The interaction of molybdenum oxides on the alumina surface and their reduction processes have been extensively investigated as documented in many literature reports (Massoth, 1978; Wang and Hall,1982; Lewis and Kydd, 1992; Wang *et al*., 1999; Kim *et al*., 1992; Lopez Cordero *et al*., 1991; Del Arco *et al*., 1993; Spevack and McIntyre,1993; Hu *et al.*, 1995; Suarez *et al*., 1985; Rajagopal *et al*., 1994, 1995; Okamoto *et al*., 1998(a, b); Abello *et al*., 2001; Thomas *et al*., 1982). As a general rule, alumina-supported molybdenum oxide catalysts consist of a monolayer of molybdenum oxide built up on the alumina surface. At a high molybdenum oxide content, this simple structure becomes much more complex since a tridimensional MoO_3 and an aluminum molybdate phase also coexist with the monolayer structure.

Although there are several methodologies to investigate catalyst reducibility, temperature programmed reduction remains prominent. TPR profiles of MoO_3/γ-Al_2O_3 catalyst containing variable amounts of molybdenum oxide have been previously reported (Lopez Cordero *et al*., 1991; Rajagopal *et al.* 1994; Abello *et al*., 2001; Damyanova *et al*., 2002). From these studies, good agreement in the number of peaks, reduction temperatures, final oxidation state of molybdenum and H_2 consumption can be derived from different TPR operating conditions. In addition to these parameters, the coordination of Mo^{6+} with O^{-2} ions in tetrahedral and/or octahedral coordination and the development of a tridimensional MoO_3 phase are often used to assign the peaks of TPR profiles. However, a detailed examination of all these studies reveals some discrepancies and, in several instances, controversial interpretations. Many authors have assigned the first peak to reduction of weakly bound octahedrally coordinated Mo^{6+} species to the alumina surface into Mo^{4+} (Lopez Cordero *et al*., 1991; Rajagopal *et al.* 1994). In opposition to this interpretation, others have associated the first reduction peak to the reduction of Mo^{6+} to Mo^{5+} (Abello *et al*., 2001). The peak placed at high temperature of reduction has usually been attributed to the deep reduction of all molybdenum species, including highly dispersed tetrahedral species, strongly bound to the support. Accordingly to the above, this study was undertaken with the aim of obtaining a better understanding of the experimental temperature programmed reduction profiles of alumina supported molybdenum oxide by applying a Monte Carlo model. In particular, the focus of the discussion is based on the reduction features of the different surface MoO_x species.

II. EXPERIMENTAL

A. Sample preparation

A commercial alumina calcined at 600 °C for 3 h was used as support. This support was impregnated with an excess of an aqueous heptamolybdate (AHM, Baker reagent grade) solution. The concentration of solution was 0.005 M (pH = 5.6) and the volume of solution was chosen in order to obtain a 13 wt% MoO_3 in the final catalyst called 13Mo/γ-Al_2O_3. The excess water was removed under reduced pressure in a rotary evaporator at 60 °C, and then the impregnate was dried at 100 °C overnight. Finally, it was calcined in air at atmospheric pressure according to the following procedure: the temperature was raised linearly for 2.5 h up to 450 °C, kept constant at 450 °C for 3 h, raised linearly up to 600°C and then maintained for 5 h at 600 °C.

B. BET Specific areas

Specific areas were determined by the BET method from the nitrogen adsorption isotherms measured in a Micromeritics Accusorb 2100E instrument. Prior to adsorption, the samples (0.200 g) were degassed at 200 °C under high vacuum for 2 h.

C. Chemical composition

Molybdenum content was determined by atomic absorption spectroscopy. The sample was subjected to alkali fusion with $KHSO_4$ and then disolved in diluted HCl solution. The measurements were carried out using a Varian AA275 spectrometer previously calibrated with standard solutions.

D. X-ray Diffraction

XRD diffraction patterns were obtained with a Rigaku diffractometer operated at 30 kV and 20 mA using Ni-filtered CuKα radiation (λ = 0.15418 nm). The powder sample was analyzed without previous treatment after deposition on a quartz sample holder. The identification of crystalline phases was made by using references from the JCPDS files.

E. X-ray photoelectron spectroscopy

The XP spectra were recorded with a VG 200 R spectrometer equipped with a Mg Kα X- ray excitation source ($h\nu$ = 1253.6 eV) operated at 12 kV and 10 mA and a hemispherical electron analyzer. The residual pressure inside the analysis chamber was kept at values below $7 \cdot 10^{-9}$ mbar. Mo3d, Al2p and C1s emissions were recorded for each catalyst. All spectra were fitted after removal of a sigmoid background. The Mo 3d signal shapes were analyzed as a set of doublets separated by defined binding energy scale, intensity contribution, position and width. All binding energies were determined by fitting the experimental curve to a Gaussian -Lorentzian peak shape with spin orbital pair intervals set at 3.15 eV and a spin-orbit area ratio of 1.5. These constraints ensure that the results make physical sense.

F. Raman spectroscopy

The Raman spectra were obtained from a single monochromator Renishaw System 1000 equipped with a cooled CCD detector (-73 °C) and a holographic super-Notch filter. The holographic Notch filter filters the elastic scattering while the intensity of the signal remains high. The sample was excited with the 514 nm Ar line, the spectrum resolution was better than 2 cm^{-1} and the spectrum acquisition consisted of five accumulations of 60 s. The spectrum was acquired under dehydrated conditions at 473 K.

G. Temperature-programmed reduction

TPR experiments were carried out in a conventional apparatus which consists of a gas handling system with mass flow controllers (Matheson), a tubular reactor, a linear temperature programmer (Omega, model CN 2010), a PC for data retrieval, a furnace and various cold traps. In each experiment the sample size was ca. 100 μmol of Mo to assure a good resolution for the experimental conditions used. Before each run, the sample was oxidized in a 30 ml min^{-1} flow of 20 vol % O_2 in He at 450 °C for 30 min. After that, helium was admitted to remove oxygen and the system cooled at 50 °C. The sample was subsequently contacted with a 30 ml min^{-1} flow of 10 vol % H_2 in Ar and heated, at a rate of 10 °C min^{-1}, from 50 °C to a final temperature of 715 °C and held for 2 h. H_2-consumption was monitored by a TCD after removing the water formed. Each TPR run was performed twice and the reproducibility was verified. The characteristic number P proposed by Malet and Caballero (1988) defined as $\beta S_o/V^*C_o$, where S_o is the initial amount of reducible species in the sample (μmol), V* is the total flow rate (ml min^{-1}), C_o the initial hydrogen concentration in the feed (μmol ml^{-1}) and β the heating rate (°C min^{-1}) was 8.7 °C in order to obtain an unperturbed reduction profile. The area under the curve was integrated to determine the H_2 consumed previous calibration.

III. RESULTS AND DISCUSSION

A. Characterization

The main characteristics of the catalyst are shown in Table 1. It can be seen that the Mo content (12.7 wt % MoO_3), as determined by AAS, is lower than the theoretical amount required to fulfill one monolayer of MoO_3 (16.7 wt % MoO_3, Abello *et al.*, 2001). The specific surface area expressed per gram of sample decreases after Mo impregnation but no changes in the specific surface area per gram of support were found. MoO_3 contributes only to the mass of the catalysts covering partially the support surface. The X-ray diffraction profile of the oxidized sample reveals the typical pattern of γ-Al_2O_3 (JCPDS 10-425); in no case diffraction lines of MoO_3 and $Al_2(MoO_4)_3$ phases were detected. The H_2-reduced sample showed a dark blue color, however, in spite of this color change, the X-ray diffraction pattern was virtually coincident with that of the oxidized counterpart. The Raman spectrum of the oxidized sample exhibited bands at 1001 and 867 cm^{-1} which correspond to the terminal Mo=O bond surface and Mo-O-Mo bridge bond, respectively (Hu *et al.*, 1995). No bands at 817 cm^{-1} and 380 cm^{-1} corresponding to crystalline α-MoO_3 and $Al_2(MoO_4)_3$ were observed. This is consistent with the X-ray diffraction results and it suggests that MoO_x exists as two-dimensional domains.

The experimental TPR profile of the 13Mo/γ-Al_2O_3 sample is shown in Fig.1.This profile exhibits two well-resolved reduction peaks. The maximum H_2-consumption in the first reduction peak is placed at 452 °C, while the second one appears just at the end temperature of the ramp (>700 °C). No significant effects of H_2 reduction were observed below 300 °C. The extent of reduction has been characterized by the change in the average oxidation number of Mo, ΔON, which depends on the amount and the reducibility of Mo species and on the experimental conditions of TPR. Thus, ΔON = 2 indicates an average reduction of Mo^{6+} to Mo^{4+}. Table 1 shows the corresponding ΔON calculated from the whole TPR profile. Assuming the initial oxidation state to be 6+, which is in agreement

with XPS results shown below, the ΔON value suggests that the average molybdenum oxidation state after the TPR run is close to 4+. In Fig.2, the XP spectra of Mo3d core-levels are shown for the oxidized and reduced samples. As judged from the binding energies of the two components of the Mo3d doublet of the oxidized sample, Fig. 2a, it can be inferred that molybdenum is present in one oxidation state (Mo^{6+}), as identified by the binding energies at 233.2 and 236.4 eV for the Mo $3d_{5/2}$ and Mo $3d_{3/2}$ components, respectively. The binding energies of the Mo 3d doublet, which are summarized in Table 2, agree well with most of the values given in the literature (Peeters *et al*., 1998; Grunert *et al*., 1992; Oliveros *et al*., 1997; De Canio *et al*., 1989; Noguera *et al*., 2000; Bañares *et al*., 1993). Once the initial chemical state of molybdenum was determined, the sample was transferred from the analysis chamber to the pretreatment chamber of the electron spectrometer and then exposed to an atmosphere of pure H_2 for 1 h at 500 °C. The reduction temperature was chosen taking into account the minimum H_2 consumption between the first and the second TPR peaks. Subsequently, the reduced sample was transferred to XPS chamber and the measurement reveals the appearance of Mo^{5+} species which are characterized by the binding energies of Mo $3d_{5/2}$ and Mo $3d_{3/2}$ peaks at 232.4 and 235.7 eV, respectively (Fig. 2b). Some authors (Grunert *et al*., 1992; Oliveros *et al*., 1997) have reported two binding energy values for Mo^{+4}: a high binding energy value (Mo $3d_{5/2}$ 231.5 - 232 eV) attributed to ionic "isolated" Mo^{+4} and a low binding energy value (Mo $3d_{5/2}$ ca. 230 eV) typically associated with Mo^{+4} as in MoO_2 and ascribed to paired double–bonded Mo^{+4}. Then, it could not rule out that Mo3d doublet attributed to Mo^{+5} is in fact a convolution of the contribution from Mo^{+5} and ionic Mo^{+4}. The relative abundance of each Mo oxidation state is estimated by dividing the Mo 3d area for a given oxidation state by the total area of the Mo 3d envelope. The fraction of unreduced Mo^{6+} is about 54 %. Although the extent of reduction determined under isothermal conditions does not coincide with that obtained under the conditions used in TPR experiments, this observation is relevant because it allows us to assume that the first reduction step consists of the reduction of Mo^{6+} to Mo^{5+}. If an important contribution of ionic Mo^{+4} was the responsible of the Mo 3d doublet, the change in the average oxidation number of Mo after TPR experiment should be higher than 2. Then, it is assumed that only Mo^{+5} contributes to the Mo3d doublet. From peak intensities and tabulated atomic sensitivity ratios (Wagner *et al*.,1981), the Mo/Al surface atomic ratios were computed for the oxidized sample and reduced samples.

These Mo/Al ratios are also included in Table 2. The XPS Mo/Al ratio is higher than the nominal value (0.051), which agrees with the high dispersion of molybdenum species which does not change after hydrogen treatment.

Taking into account the above results, the TPR profile was simulated by a Monte Carlo method. A precise description of the MC methodology has been given elsewhere (Binder, 1997; Rudzinsky *et al*., 1996; Zhdanov, 1991).

B. Simulation Model

A Monte Carlo approach has been developed to analyze the experimental TPR profiles of the $13Mo/\gamma\text{-}Al_2O_3$ sample. Under moderate temperatures of reduction used in this work, two peaks are observed which correspond to the reduction of different Mo species on the $\gamma\text{-}Al_2O_3$ surface. It is well known that different MoO_x domains are present on alumina from isolated monomolybdate to two-dimensional polymolybdate and three dimensional MoO_3 cluster, scheme I (Fig. 3).

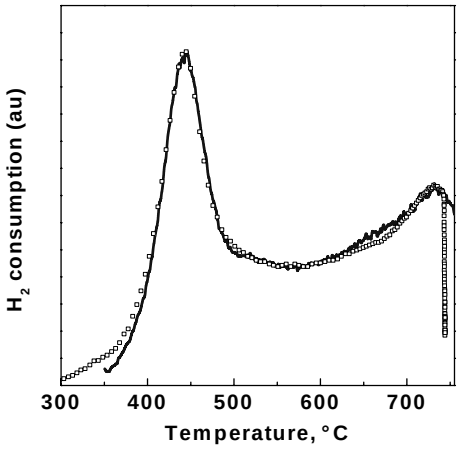

Figure 1. TPR profile of $13Mo/\gamma Al_2O_3$. (° Experimental data; — simulated data).

Table 1. Main characteristics of $Mo/\gamma\text{-}Al_2O_3$ catalyst

Sample	%MoO_3 AAS	S_{BET} $m^2g^{-1}{}_{cat}$	S_{BET} $m^2g^{-1}{}_{sup}$	XRD phases	Raman bands cm^{-1}	ΔON
$13Mo/\gamma\text{-}Al_2O_3$	12.7	166.0	190.0(*)	$\gamma\text{-}Al_2O_3$	1001, 867	2.23

(*) S_{BET} $\gamma\text{-}Al_2O_3$ = 184.6 m^2 g^{-1}

Table 2. Binding Energies of Mo 3d core-level and surface atomic ratios of oxidized and reduced $Mo/\gamma\text{-}Al_2O_3$ catalyst

Catalyst state	Binding Energy, eV		$(Mo/Al)_{atom}$
	$Mo_{3d3/2}$	$Mo_{3d5/2}$	
Oxidized	236.4 (2.3)	233.2(2.3)	0.100
Reduced in H_2 at	236.5 (2.2)	233.4 (2.2)	0.098
500 °C	235.7 (2.6)	232.4 (2.6)	

fwhm values are given in parenthesis

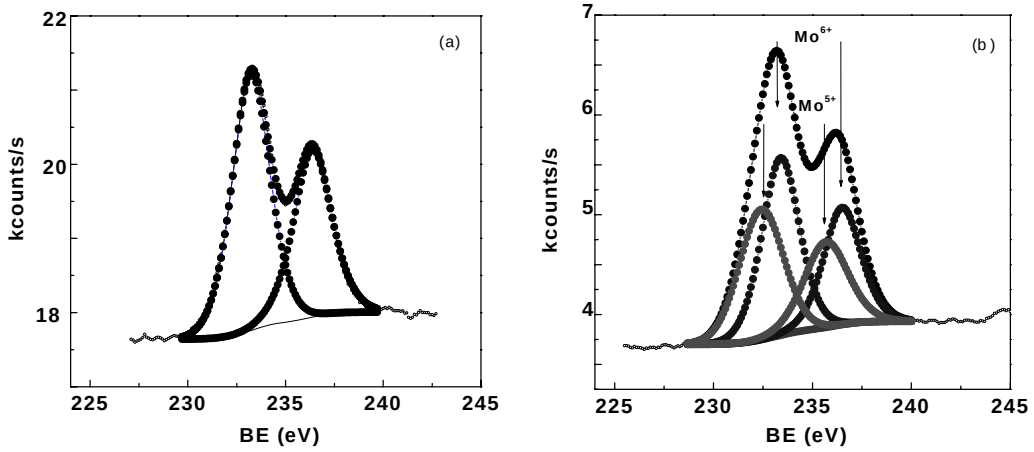

Figure 2. The XP spectra of Mo3d core level of (a) oxidized sample; (b) reduced sample in H_2 at 500°C for 1 h.

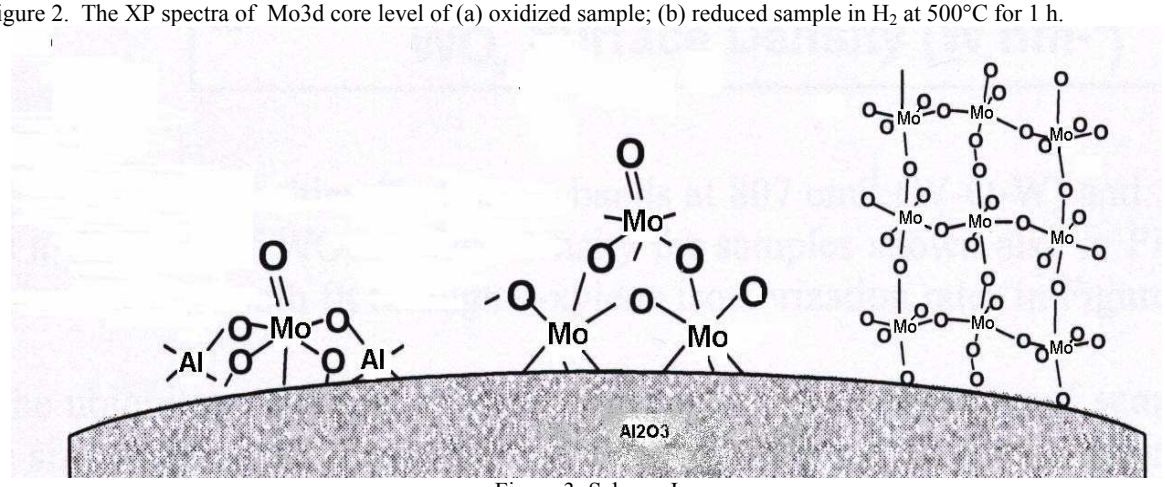

Figure 3: Scheme I

Scheme II Scheme III

Figure 4: Schemes I and III

Evidence for the structural evolution has been provided by Raman spectroscopy combined XANES (Hu *et al*., 1995; Abello ,2002).

Taking into account that on our sample MoO_3 is not detected by Raman, the model only considers two different structures on γ-Al_2O_3. A larger fraction of Mo species is in the polymeric form (which will be represented into the text by scheme II, Fig. 4), and a minor fraction of Mo species forms highly dispersed monomeric structures (which will be represented by scheme III, Fig. 4). A linear distribution of oxygen sites for the Mo-O-Mo bridge is considered for polymeric structures and a bidimensional distribution of oxygen sites for Mo=O in monomeric species.

The interaction of the various Mo-O locations with hydrogen is proposed to imply the following reactions. Three different kinetics are considered for polymeric structures assuming a different extent of surface oxygen reducibility.

The first reaction takes place on the surface oxygen shared by two Mo^{6+} ions:

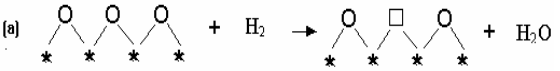

where □ represents an oxygen vacancy. The second reaction occurs from a surface oxygen shared by Mo^{5+} and Mo^{6+}:

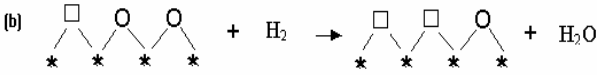

The third reaction occurs from a surface oxygen shared by Mo^{5+} and Mo^{5+}:

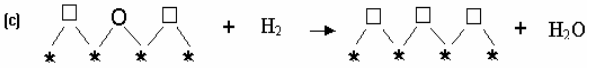

The three reactions lead to water formation. Reaction (a) reduces Mo^{6+} to Mo^{5+}, the second one generates Mo^{5+} and Mo^{4+} and the last one only produces Mo^{+4}.

For reduction of monomeric structures the model assumes four different kinetics. They are schematically depicted as follow:

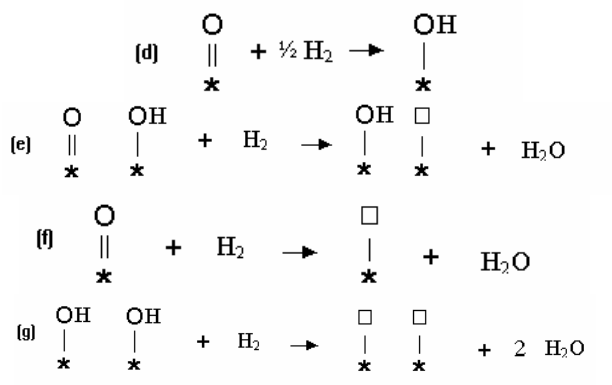

Reaction (d) reduces Mo^{6+} to Mo^{5+} and leads to the formation of surface OH. Reactions (e), (f) and (g) lead to the formation of one (reactions e and f) or two (reaction g) water molecules. Reaction (e) reduces two groups from Mo^{+6} and Mo^{+5} to Mo^{+5} and Mo^{+4}, respectively. Reaction (f) leads to the reduction of Mo=O from Mo^{+6} to Mo^{+4} and the last one only produces two oxygen vacancies (Mo^{+4}) from two Mo-OH groups.

In order to perform the simulation, a system consisting of N surface reactive sites (5×10^6) was taken into account (Rudzinsky *et al*., 1996; Zhdanov, 1991). It was assumed that the polymeric to monomeric concentration ratio was 2.3 (70% of polymeric and 30% of monomeric) (Abello, 2002; Shimada *et al*, 1992). The initial oxidation state for all molybdenum species was considered to be 6+ in agreement with XPS results.

The simulation scheme was performed according to the following steps:

(i) Definition of the surface of N sites and fixing an initial temperature $T_0 = 300$ °C.

(ii) A given site "i" in the lattice is chosen at random.

(iii) The reduction process is tested on each site "i" by comparing the probability of each reaction (P_r) with a random number ξ ($0 \leq \xi \leq 1$). The reaction probability is given by the expression

$$Pr = \nu(r) \cdot \exp(E_a(r, i)/RT) \cdot \Delta T/\beta$$

where $\nu(r)$ is the pre-exponential factor for reaction "r"; $E_a(r, i)$ is the activation energy for reaction "r" on "i" site; β is the heating rate, R is the gas constant and ΔT is the temperature increment.

All the seven (a-g) reactions participate with an equivalent weight according to probability. If the random number (ξ) results greater than the probability (P_r) for the r reaction occurrence, this reaction is not selected and the site reduction is considered as a null event. The simulation follows the steps:

(iv) Before the temperature is increased, the number of times that the reaction is selected, the H_2 consumption, the water production, the amount of surface OH and the reduction state of all sites are estimated.

(v) Increase the temperature by ΔT and repeat from step (ii) until the surface is completely reduced or the temperature reaches 800°C.

The simulation process allows one to determine the activation energy of each reduction kinetics step and the population of both structures. The normal distribution of activation energy and the temperature in the peak maximum are shown in Table 3. The relative intensity of the two peaks after simulation is in very good accordance with that obtained from the experimental TPR profile.

In Fig. 5(i), the H_2 consumption and the three peaks corresponding to each reaction for the polymeric structure are shown. The H_2 consumption agrees with the production of water. The maximum temperature of three peaks are 443°, 657° and 734°C. In Fig. 5(ii), the behavior of monomeric species against the reduction is shown. In this case, the H_2 consumption is the sum of the four peaks with maximum temperatures at 511°, 550°, 551°, and 599 °C. It can be noted that the H_2 consumption curve does not coincide with the water formation curve because of the appearance of surface OH in the first step of reduction.

The presence of Mo-OH groups can explain the increase of Brønsted acidity found on reduced molybdena-alumina samples. Suarez *et al*. (1985) have reported that reduction of Mo/Al_2O_3 catalysts with hydrogen causes the total acidity to increase to a maximum and then to decrease as the sample is reduced further. The increase in total acidity is caused by a slight increase in Brønsted acidity and a larger increase in the Lewis acidity. The initial increase in Lewis acidity may be due to generation of anion vacancies on molybdenum. These changes studied by infrared spectroscopy and thermo-gravimetric analysis of adsorbed pyridine are in line with the present model (Suarez *et al.*, 1985). Figure 1 shows the global behavior of both species. The agreement between experimental and simulated data is satisfactory. From the evolution of oxidation state of surface Mo, Fig. 6, it is seen that the reduction of Mo species starts at 375 °C.

Table 3. Simulation results

Structure	Reaction	E_{act} [kJ mol^{-1}]	σ [kJ mol^{-1}]	T_{peak}[°C]
I	a	122.9	6.7	443
	b	181.8	9.2	657
	c	198.6	10.5	734
II	d	161.3	12.5	511
	e	188.1	16.7	551
	f	188.1	16.7	550
	g	188.1	12.5	599

σ standard deviation

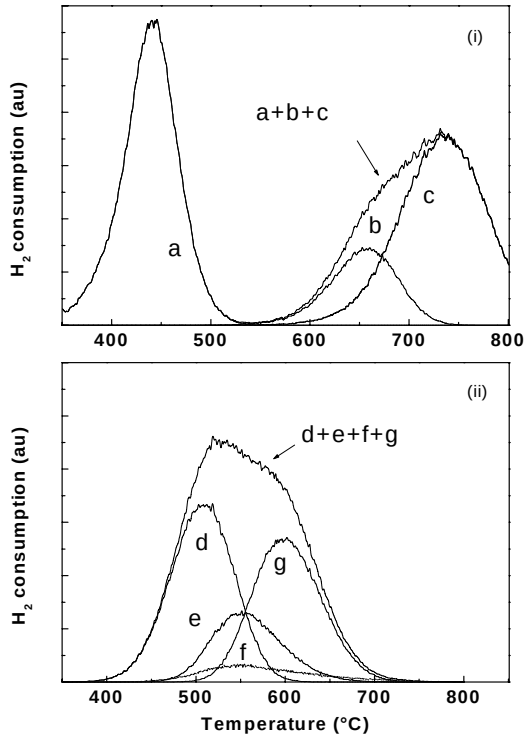

Figure 5. Hydrogen consumption for the reduction process of MoO_x on γ-Al_2O_3 corresponding to (i) polymeric and (ii) monomeric species according to reaccions a, b, c, d, e, f and g.

50% of the Mo^{6+} is reduced to Mo^{5+} at 460 °C. At 500°C, 30% of Mo species is still in oxidation state 6+. The difference in population of Mo^{6+} between XPS and TPR results can be attributed to differences in the reduction regime, sample treatment (use of H_2/Ar mixture instead of pure H_2), different reduction time, different sample forms and flow regimes. The Mo^{6+} ions completely disappear at 725 °C where around 60% of Mo^{4+} coexists with about 40% of Mo^{5+}. The maximum fraction of Mo^{5+} species can be obtained at 550 °C.

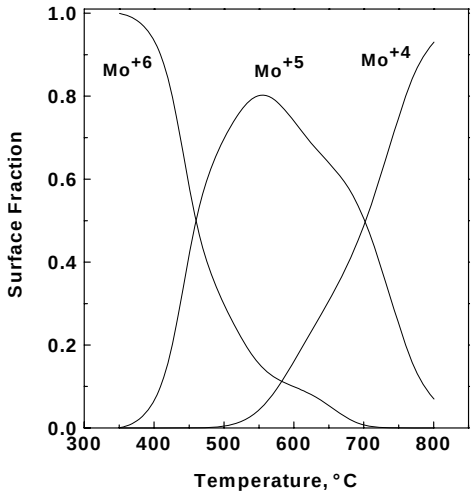

Figure 6. Evolution of oxidation state of surface Mo on γ-Al_2O_3 under temperature programmed reduction

IV. CONCLUSIONS

A Monte Carlo approach to describe the reduction profiles of bidimensional MoO_x structures grown on an alumina sustrate was developed. From the analysis of the experimental and simulated results, the first TPR peak can be assigned to the reduction of polymeric Mo species mainly from 6+ to 5+, while the second peak can be attributed to the reduction of all Mo species to Mo^{4+} including the monomeric species from 6+ to 4+. The knowledge of the oxidation state evolution of molybdenum with temperature in the presence of hydrogen allows one to control the initial reduction extent of surface which has a significant effect on the properties of the catalyst.

ACKNOWLEDGMENTS

The authors wish to thank Dr. M.A. Bañares for Raman assistance. Financial support is acknowledged to CONICET, to Universidad Nacional de San Luis and Universidad Nacional de La Plata.

REFERENCES

Abello, M.C., Doctoral Thesis, Facultad de Ingeniería, Universidad Nacional de La Plata (2002).

Abello, M.C., M.F. Gomez and O. Ferretti, "Mo/γ-Al_2O_3 catalysts for the oxidative dehydrogenation of propane. Effect of Mo loading," *Appl. Catal. A: General* **207**, 421-431 (2001).

Bañares, M.A., J.L.G. Fierro and J.B. Moffat, "The Partial Oxidation of Methane on MoO_3/SiO_2 Catalysts: Influence of the Molybdenum Content and Type of Oxidant," *J. Catal.* **142**, 406-417 (1993).

Binder, K., **"**Applications of Monte Carlo methods to statistical physics," *Rep. Prog. Phys*. **60**, 487-560 (1997).

Damyanova, S., L. Petrov, M.A. Centeno and P. Grange, "Characterization of molybdenum hydrodesulfurization catalysts supported on ZrO_2-Al_2O_3 and ZrO_2-SiO_2 carriers," *Appl. Catal. A: General* **224**, 271-284 (2002).

De Canio, S., M. Cataldo, E. De Canio and D. Storm, "Evidence from XPS for the stabilization of high-valent molybdenum by addition of potassium in Mo/Al_2O_3 catalysts," *J. Catal*. **119**, 256-286 (1989).

Del Arco, M., S.R. Carrazán, V. Rives, F.J. Gil-Llambías and P. Malet, "Surface Species Formed upon Supporting Molybdena on Alumina by Mechanically Mixing Both Oxides," *J. Catal.* **141**, 48-57 (1993).

Grunert, W., A. Y. Stakheev, W. Morke, R. Feldhaus, K. Anders, E.S. Shapiro and K.M. Minachev, "Reduction and metathesis activity of MoO_3/Al_2O_3 catalysts: I. An XPS investigation of MoO_3/AI_2O_3 catalysts," *J. Catal.* **135**, 269-286 (1992).

Hu, H., I.E. Wachs and S. Bare, "Surface structures of supported molybdenum Oxide Catalysts: Characterization by Raman and Mo L_3-Edge XANES," *J. Phys. Chem.* **99**, 10897-10910 (1995).

Kim, D., K. Segawa, T. Soeya and I. Wachs, "Surface structures of supported molybdenum oxide catalysts under ambient conditions," *J. Catal.* **136**, 539-553 (1992).

Lewis, J.M. and R.A. Kydd, "The MoO_3-Al_2O_3 interaction: Influence of phosphorus on MoO_3 impregnation and reactivity in thiophene HDS," *J. Catal*. **136,** 478-486 (1992).

Lopez Cordero, R., F.J. Gil Llambias and A. Lopez Agudo, "Temperature programmed reduction and zeta potential studies of structure of MoO_3/Al_2O_3 and MoO_3/SiO_2 catalysts. Effect of the impregnation pH and molybdenum loading," *Applied Catal. A: General* **74**, 125-136 (1991).

Malet, P. and A. Caballero, "The selection of experimental conditions in temperature-programmed reduction experiments," *J. Chem. Soc. Faraday Trans.* **84**, 2369-2375 (1988).

Massoth, F.E., "Characterization of molybdena catalysts," *Adv. Catal*. **27**, 265-309 (1978).

Noguera, O., J. Sarrín, M.R. Goldwasser, C. Pfaff, P. Betancourt, M.J. Perez Zurita, C. Scott, J. Goldwasser and M. Houalla, "Estudio de la reducubulidad de catalizadores molibdeno-Alumina," *Proc. of the XVII Iberoamerican Symposium on Catalysis*, Porto, Portugal,197 (2000).

Okamoto, Y., Y. Arima, K. Nakai, S. Umeno, N. Katada, H. Yoshida, T. Tanaka, M. Yamada, Y. Akai, K. Segawa, A. Nishiijima, H. Matsumoto, M. Niwa and T. Uchijima, "A study on the preparation of supported metal oxide catalysts using JRC-reference catalysts. I. Preparation of a molybdena–alumina catalyst. Part 1. Surface area of alumina," *Appl. Catal. A: General* **170**, 315-328 (1998a).

Okamoto, Y., Y. Arima, M. Hagio, K. Nakai, S. Umeno, Y. Akai, K. Uchikawa, K. Inamura, T. Ushikubo, N. Katada, S. Hasegawa, H. Yoshida, T. Tanaka, T. Isoda, I. Mochida, K. Segawa, A. Nishiijima, M. Yamada, H. Matsumoto, M. Niwa and T. Uchijima, "A study on the preparation of supported metal oxide catalysts using JRC-reference catalysts. I. Preparation of a molybdena–alumina catalyst. Part 2. Volume of an impregnation solution," *Appl. Catal. A: General* **170**, 329-342 (1998b).

Oliveros, I., M.J. Perez Zurita, C. Scott, M.R. Goldwasser, J. Goldwasser, S. Rondon, M. Houalla and D.M. Hercules, "The Isomerization of Cyclopropane over Reduced Molybdena–Alumina Catalysts," *J. Catal.* **171**, 485-489 (1997).

Peeters, I., A. Denier van des Gon, M.A. Reijme, P. J. Kooyman, A. M. de Jong, J. van Grondelle, H. H. Brongersma and R.A. van Santen, "Structure–Activity Relationships in the Ammoxidation of Ethylene in the Absence of Molecular Oxygen over γ-Al_2O_3-Supported Molybdenum Oxide Catalysts," *J. Catal.* **173**, 28-42 (1998).

Rajagopal, S., H.J. Marini, J.A. Marzari and R. Miranda, "Silica-Alumina-Supported Acidic Molybdenum Catalysts - TPR and XRD Characterization," *J. Catal.* **147**, 417-428 (1994).

Rajagopal, S., J.A. Marzari and R. Miranda, "Silica-Alumina-Supported Mo Oxide Catalysts: Genesis and Demise of Brønsted-Lewis Acidity," *J Catal*. **151**, 192-203 (1995).

Rudzinsky, W., W.A. Steele and G. Zgrablich, *Equilibria and dynamics of gas adsorption on heteregeneous surfaces*, Elsevier, Amsterdam (1996).

Shimada, H., N. Matsubayashi, T. Sato, Y. Yoshimura, A. Nishuima, N. Kosugi and H. Kuroda, "XAFS study of molybdenum oxide catalysts on various supports," *J. Catal.* **138**, 746-749 (1992).

Spevack, P. and N.S. McIntyre, "A Raman and XPS investigation of supported Molybdenum oxide thin films. 1. Calcination and reduction studies," *J. Phys. Chem*. **97**, 11020-11030 (1993).

Suarez, W., J. Dumesic and Ch. Hill, "Acidic properties of molybdena-alumina for different extents of reduction: Infrared and gravimetric studies of adsorbed pyridine," *J. Catal.* **94**, 408-421 (1985).

Thomas, R., E. Van Oers, V. De Beer, J. Medema and J. Moulijn, "Characterization of γ-alumina-supported Molybdenum oxide and tungsten oxide; reducibility of the oxidic state versus hydrodesulfurization activity of the sulfided state," *J. Catal.* **76**, 241-253 (1982).

Wagner, C. D., L. E. Davis, M. V. Zeller, J. A. Taylor, R. H. Raymond and L.H. Gale, "Spectroscopy for Chemical Analysis," *Surf. Interface Anal.* **3**, 211-225 (1981).

Wang, L. and W. K. Hall, "The preparation and genesis of molybdena-alumina and related catalyst systems," *J. Catal*. **77**, 232-241 (1982).

Wang, X., B. Zhao, D. Jiang and Y. Xie, "Monolayer dispersion of MoO_3, NiO and their precursors on γ-Al_2O_3," *Appl. Catal. A: General* **188**, 201-209 (1999).

Zhdanov, V. P., *Elementary phycochemical processes on solid surfaces*, Plenum Press, New York (1991).

Received: November 28, 2005
Accepted: June 9, 2006
Recommended by Subject Editor: Ana Lea Cukierman